
Large-Eddy Simulation of a Turbulent Flow around a Multi-Perforated Plate

Simon Mendez¹, Franck Nicoud¹, and Thierry Poinsot¹

CERFACS, 42, avenue Gaspard Coriolis. 31057 Toulouse cedex 1. France.
mendez@cerfacs.fr

Abstract

Key words: Effusion cooling, LES, DNS, Wall modeling for RANS, Gas turbines

The film cooling technique is often used to protect the hot components in gas turbines engines by introducing cold air through small holes drilled in the wall. The hot products are mixed with the injected gas and the temperature in the vicinity of the wall is reduced. Classical wall functions developed for impermeable walls and used in Reynolds-Averaged Navier-Stokes methods cannot predict momentum/heat transfer on perforated plates because the flow is drastically modified by effusion. In order to obtain a better understanding of the flow structure and predominant effects, accurate simulations of a turbulent flow around an effusion plate are reported. Large-Eddy Simulations of the flow created by an infinite multi-perforated plate are presented. The plate is perforated with short staggered holes inclined at an angle of 30 deg to the main flow, with a length-to-diameter ratio of 1.73. Injection holes are spaced 6.74 diameters apart in the spanwise direction and 5.84 diameters apart in the streamwise direction. Results for mean velocity and velocity fluctuations are compared with measurements made on the LARA large-scale isothermal experiment [1].

1 Introduction

In almost all the systems where combustion occurs, solid boundaries need to be cooled. One possibility often chosen in gas turbines is to use multi-perforated walls to produce the necessary cooling [2]. In this approach, fresh air coming from the casing goes through the perforations and enters the combustion chamber [3]. The associated micro-jets coalesce to give a film that protects the internal wall face from the hot gases. The number of submillimetric holes is far

too large to allow a complete description of the generation/coalescence of the jets when computing the 3D turbulent reacting simulation within the burner. Effusion is however known to have drastic effects on the whole flow structure, noticeably by changing the flame position. This is shown in Fig. 1, where the temperature fields from two RANS computations of a TURBOMECA configuration are compared. The code used for these simulations is N3S-Natur, widely used by TURBOMECA for calculating the flow in combustion chambers. The images shown are cuts of the combustion chamber with a perforated wall zone. Two different models are used to reproduce the effect of effusion cooling on the main flow: in Fig. 1.a, a simple model using a uniform injection is used to inject the correct mass flow rate in the combustion chamber while in Fig. 1.b, an ad hoc model is used.

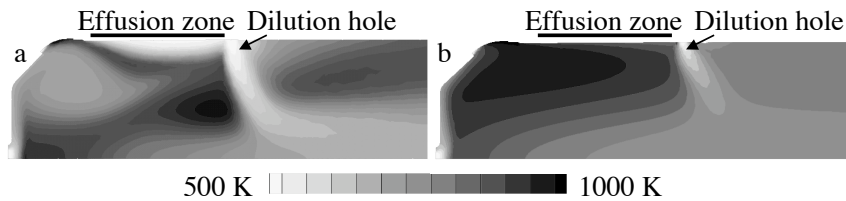


Fig. 1. Temperature fields from RANS computations using two different models to reproduce effusion cooling. a: simple model imposing the correct mass flow rate without any additional treatment. b: ad hoc model developed by TURBOMECA. Results from TURBOMECA simulations.

It is obvious that the model used to mimic the effect of effusion cooling has a huge effect on the general topology of the flow: the position of the zone of high temperature is completely changed between Fig. 1.a and Fig. 1.b, showing that the position of the flame is completely different. As a consequence, new wall functions for turbulent flows with effusion are required to perform predictive full scale computations. The present study is a subset of a larger research activity whose main long term objective is to develop such appropriate and scientifically meaningful wall models

One major difficulty in developing wall functions is that the boundary fluxes depend on the details of the turbulent flow structure between the solid boundary and the fully turbulent zone. Such detailed description of the flow in the near wall region can hardly be obtained experimentally because:

- the perforation imposes small scales structures that are out of reach of current experimental devices
- the thermal conditions in actual gas turbines make any measurement very challenging.

This can explain the lack of data concerning full-coverage film cooling through discrete holes. Most of the works concerning discrete-hole film cooling

treat the case of a single row of holes (cooling application for turbine blades), and only few studies on several rows of holes are available. Most available aerodynamic measurements deal with large-scale isothermal flows [1, 3–5]. On the contrary, experimental studies about the thermal behavior (evaluation of cooling effectiveness and heat transfer coefficient at the wall) do not provide any flow measurements [6] or too coarse ones [7].

Numerical capabilities have increased during the last years: RANS simulations of full-coverage film cooling with several rows (10 rows for Harrington *et al.* [8] and 7 rows for Papanicolaou *et al.* [9]) have been performed. These simulations have proved the ability of numerical codes to reproduce effusion flows. However, the results have never been analyzed in order to build a wall model for effusion plates. Moreover, as long as only a few number of rows are considered, wall resolved LES can be performed in place of RANS calculations in order to gain insight about the jet-mainstream interaction. Large-Eddy Simulations [10, 11] on single jets in crossflow have been performed but these studies do not give any information about the interaction between jets. Moreover, numerical simulations often study the case of large hole length-to-diameter ratios, while effusion cooling for combustion chamber walls is done through short holes, because of the small thickness of the plates in aeronautical applications. This makes it necessary to compute both the aspiration and the injection sides of the perforated plate.

In order to obtain precise information about the behavior of the flow near a perforated plate, Large-Eddy Simulations (LES) are performed: Direct Numerical or Wall-resolved Large-Eddy Simulations can be used to generate precise and detailed data of generic turbulent flows under realistic operating conditions, with no limitations due to the size of the configuration or to difficulties to realize measurements in a hot flow. In this paper, a computational methodology is proposed to perform calculations of an effusion flow and results are presented. They are compared with the LARA experimental database, provided by TURBOMECA, that deals with a large-scale isothermal plate.

2 Computational Methodology

2.1 How To Study Effusion Cooling

The objective is to gain precise information about the behavior of the flow around a multi-perforated wall. In a whole configuration, the jets created by effusion interact with the main flow in the combustion chamber. This main flow is turbulent and many effects have to be taken into account to describe it. But since the aim is to focus on the flow near the wall, it is not necessary to compute the main flow as it is in a combustor. For practical studies of effusion cooling, experimental test rigs are generally divided into two channels: one represents the combustion chamber, with a primary flow of hot

gases and the other represents the casing, with a secondary flow of cooling air. Several rows of several holes are drilled into the plate that separates the two channels in order to observe the interaction between jets. Because the pressure is higher in the casing side, some air is injected through the perforated plate. For numerical simulations, like in experiments, this simplified configuration is used.

2.2 From The Experimental Studies To The Numerical Calculations

Results in the open literature show that the effusion flow highly depends on the configuration of interest: the flow generated by a ten-row plate would be different from the one generated by a twenty-row plate. This situation is hardly tractable from a modeling point of view and we decided to simplify the problem by considering the asymptotic case where the number of rows is infinitely large. The simulation is then designed to reproduce this asymptotic case of a turbulent flow with effusion around an infinite plate. This choice presents several advantages:

- The infinite plate can be reduced to a domain containing only one perforation, with periodic boundary conditions to reproduce the whole geometry of an infinite plate, as it is suggested in Fig. 2.
- The difficult question of the inlet and outlet boundary conditions in turbulent simulations (see [12]) is avoided.

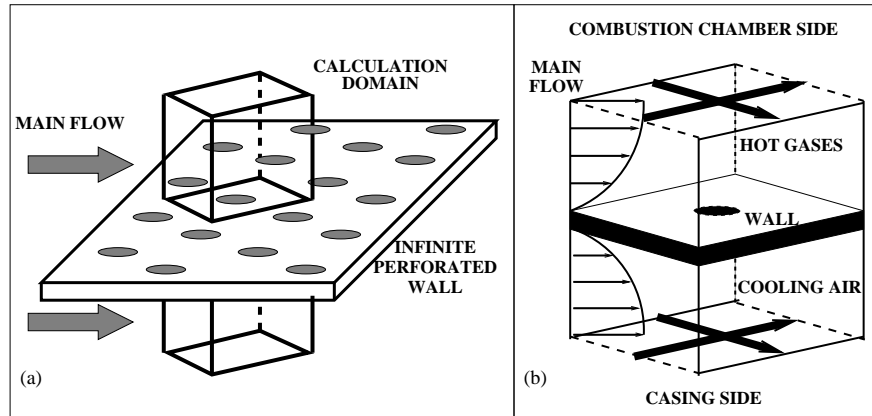


Fig. 2. From the infinite plate to the "bi-periodic" calculation domain. (a) Geometry of the infinite perforated wall. (b) Calculation domain centered on a perforation; the bold arrows correspond to the periodic directions.

With such a periodic calculation domain, the objective is to have information about the structure of the flow far from the first rows, when the film

is established. However, this periodic option raises a problem: natural mechanisms that drive the flow, such as pressure gradients, are absent. The flow has to be generated artificially.

2.3 Generation Of A Periodic Flow With Effusion

Main Flows

For a classical channel flow, a volumetric source term is added to the momentum conservation equation in order to mimic the effect of the mean streamwise pressure gradient that would exist in a non-periodic configuration. This is a very classical method for channel or pipe flow simulations. The source term is usually constant over space. For example, it can have the following form:

$$S_{(\rho U)} = \frac{(\rho U_{target} - \rho U_{mean})}{\tau} \quad (1)$$

The source term compares a target for momentum, ρU_{target} , with the average momentum in the channel, ρU_{mean} . A relaxation time τ characterizes the rapidity with which ρU_{mean} tends towards its target value. Naturally, this treatment is done for one channel. This approach can be generalized in the case of an effusion configuration, having a source term of the previous form for each channel: therefore, the source term on momentum is constant by part, with two distinct values for the cold and the hot sides. No source term is applied in the hole itself.

Injection

In experiments, channels are bounded by impermeable walls at the top and at the bottom. If used in conjunction with periodic boundary conditions in the tangential directions, this outer condition prevents the flow from reaching a statistically steady state with effusion, because the net mass flux through the perforation tends to eliminate the pressure drop between the cold and the hot domains. In order to sustain the secondary effusion flow in periodic LES, two different strategies were investigated [13].

- Constant Source Terms strategy: impermeable boundary conditions are kept at the top and the bottom of the computational domain, but source terms are added to the mass and energy equations in order to drive the mean pressure and temperature towards reference values, consistent with effusion.
- Boundary Conditions strategy: the Navier-Stokes equations are solved without any additional source term, but characteristic-based [14] freestream boundary conditions are used at the top and bottom ends of the domain in order to impose the appropriate mean vertical flow rate.

Both approaches are detailed in [13] and prove to give very similar results. Results from the second method (Boundary Conditions strategy) are discussed in this paper.

3 Details Of Numerical Simulations

The configuration that is considered in this paper corresponds to the geometry studied by Miron [1]. The study focuses on the case of a large-scale isothermal plate, with a hole diameter fixed at $d=5$ mm (0.5 mm is the common value for gas turbines applications). The spacing between the holes correspond to the classical industrial applications: holes are spaced 6.74 diameters apart in the spanwise direction and 5.84 diameters apart in the streamwise direction. The thickness of the plate is 10 mm and holes are angled at 30 deg with the plate: they are short holes, with a length-to-diameter ratio of 1.73.

The computational domain is designed as the smallest domain that can reproduce the geometry of an infinite plate with staggered perforations, as it is shown in Fig. 2. All simulations are carried out with the AVBP code [15]. It is a fully explicit cell-vertex type code that solves the compressible multi-species Navier-Stokes equations on unstructured meshes for the conservative variables (mass density, momentum and total energy). AVBP is dedicated to LES and it has been widely used and validated in the past years in all kinds of configurations. The present simulations are based on the WALE sub-grid scale model [16]. The numerical scheme is the TTGC scheme [17] (third order in time and space): this scheme was specifically developed to handle unsteady turbulent flows with unstructured meshes. The grid used for the calculations contains 1,500,000 tetrahedral cells. In this grid, fifteen points describe the diameter of the hole and on average the first off-wall point is situated at $y^+ \approx 5$. Typically the cells along the wall to be cooled and in the hole are sized to a height of 0.3 mm. This rather coarse grid is sufficient to show the ability of the method to reproduce the main features of the flow. Another grid is used in this paper in section 4.2 to evaluate the effect of the grid resolution: this is a very coarse grid with 150,000 tetrahedral cells. The results are discussed and compared to the results obtained with the first grid. The grid with 1,500,000 cells will then be called FINE and the one with 150,000 cells will be called COARSE. All the results presented, except in section 4.2, are obtained with the finer grid.

4 Results And Discussion

4.1 Operating Point

Results are presented for a typical operating point of the experimental isothermal database provided by TURBOMECA, concerning the LARA test rig. Both the primary flow, which represents the burned gases flow inside the combustion chamber, and the secondary flow, which represents the cold air coming from the compressor, are at the same temperature. The main aerodynamical parameters, given for the region up of the perforations, are summarized here:

- The Reynolds number for the primary flow (based on the duct centerline velocity and the half height of the rectangular duct) is $Re=17750$.
- The Reynolds number for the secondary flow (based on the duct centerline velocity and the half height of the rectangular duct) is $Re=8900$.
- The pressure drop across the plate is 42 Pa.
- The blowing ratio is $\tau_1 = 1.78$.

In simulations, the first three parameters are fixed. The behavior of the flow in the hole and related blowing ratio result from the calculations. Numerical results are compared with measurements performed at the ninth row of the LARA experimental test rig. Twelve rows of holes are studied in the experiment but the ninth row has been chosen to compare with numerical results because it is the location where measurements are most numerous. Further details about this experiment can be found in [1] and [18].

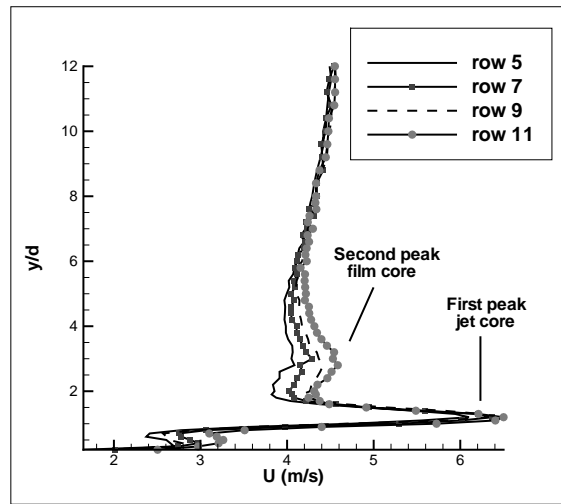


Fig. 3. Experimental measurements: mean streamwise velocity profiles evolution in the injection region.

Measurements show the formation of a film created by effusion through the plate. Jets interact together to form a film that is able to protect the plate from the primary flow (hot gases in real cases), even after the perforated zone. The film needs several rows of holes to be formed, but only the structure of the film far from the first rows are interesting for comparisons with our numerical simulations. The primary flow is disturbed in the neighborhood of the plate. Figure 3 shows the evolution of the streamwise velocity profile, 3 diameters downstream of the center of the hole at rows 5, 7, 9 and 11. After a few rows, just downstream of the hole, mean streamwise velocity profiles

are characterized by two peaks: the first one, next to the wall, represents the jet core. It is the result of the interaction between the jet coming out of the hole and the film. The second peak represents the film core, which is the result of the interaction of all former jets with the main flow. The value of the peaks behave differently: the peak related to the jet does not change a lot from one row to another, whereas the peak corresponding to the film core is highly influenced by the number of rows upstream of the position of the profile. The presence of a secondary velocity peak can be observed under the jet, for $y/d \approx 0.5$. This is the sign of a well-known phenomenon for inclined jets in crossflow: the incident flow is deflected by the jet and a part of the flow is entrained towards the wall by the effect of the rotating structure of the jet. The entrainment process has been widely discussed, and further details can be found in Tyagi and Acharya [10] and Yavuzkurt *et al.* [5].

4.2 Validation Of The Results By Comparison With Experimental Data

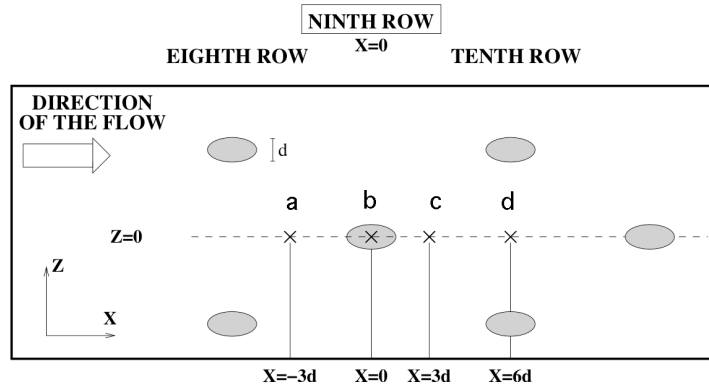


Fig. 4. Location of the profiles measured on the experimental data.

Averages are performed over a period that corresponds to twenty characteristic convection times for the primary flow. Comparisons are made with experimental profiles at locations shown in Fig. 4.

Figure 5 shows the evolution of the mean streamwise velocity profile upstream, above and downstream of the hole. Symbols correspond to measurements, lines to AVBP calculations: dotted lines are the results from the coarse grid and continuous lines are the results from the finer grid. Figure 5.a shows the flow upstream of the hole. Under $y/d=6$, the profile shows the presence of the cooling film, formed by the former injections. This profile interacts with the jet in Fig. 5.b. At $y=0$, high velocities are present at the outlet of the hole. The jet strongly modifies the profile downstream of the jet, as shown

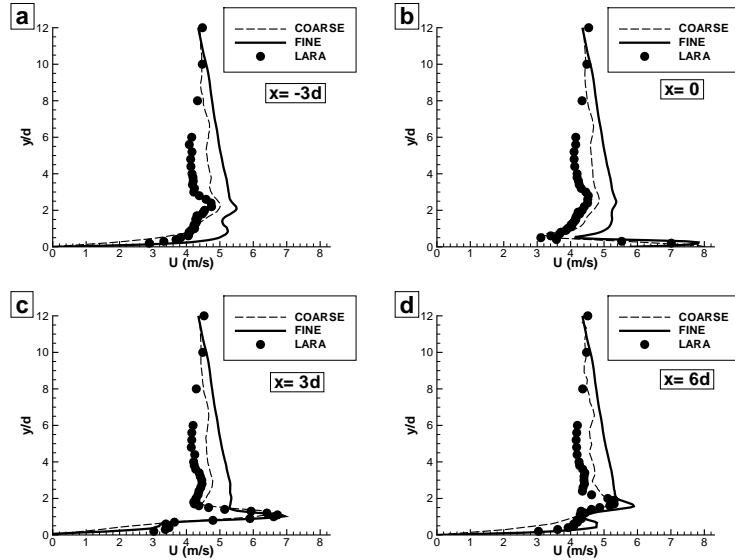


Fig. 5. Mean streamwise velocity profiles at four locations: dotted lines correspond to LES results with the coarse grid, continuous line to LES with the finer grid and symbols correspond to measurements.

in Fig. 5.c. The characteristic form of effusion profile can be observed, with a peak marking the jet just upstream, and a second peak that represents the film created by injection through the former holes. The second peak is more pronounced in the experimental and in the coarse grid results. More downstream (Fig. 5.d), the jet loses its strength and progressively coalesces with the film to add its contribution. In Fig. 5.d, the velocity near the wall increases compared to Fig. 5.c. This is an effect of the entrainment process.

A general good agreement is obtained between the simulations and the experiment. The results from the coarse grid reproduce very well the form of the profile. However, the near-wall region is not discretized finely enough: this leads to important errors on the velocity gradient. These errors are due to a bad description of the vortical structure of the flow: the entrainment process, that is a major characteristic of the flow, is not reproduced with the coarse grid.

Figure 5 shows two different trends for the finer grid: first of all, the behavior in the near-wall region seems to be quite well reproduced and the velocity peak due to the jet is situated as in the experiment. This ability to describe the near-wall region is crucial because the aim is to get information about what happens in this region, in which measurements are very difficult to perform. This time the entrainment process is reproduced nicely.

Larger differences can be found above the jet, in the film core region. It is believed that it is mainly due to the difference between the configurations that are being studied. Simulations characterize the flow around an infinite perforated plate, while measurements are made at the ninth row. This effect of accumulation for mean streamwise velocity is coherent with what is observed experimentally in Fig. 3: the number of rows has an effect on the mean velocity profile above the peak due to the jet. Then, a nine-row plate and an infinite plate cannot provide the same results and differences are coherent with Fig. 3, in which it can be observed that the velocity of the film core tends to increase with the number of rows. This accumulation effect is not reproduced in the coarse grid simulation, as the accumulation of fluid near the wall is a consequence of the entrainment process.

For quantities that are not directly affected by the effect of accumulation due to the infinite configuration, comparisons between experiments and simulations show very good agreement for the fine grid, as shown for the mean vertical velocity (top of Fig. 6) for stations c and d or for the root mean square velocities (bottom of Fig. 6). All the profiles for these quantities show the same agreement for the fine grid simulations. On the contrary the results from the coarse grid are clearly worse.

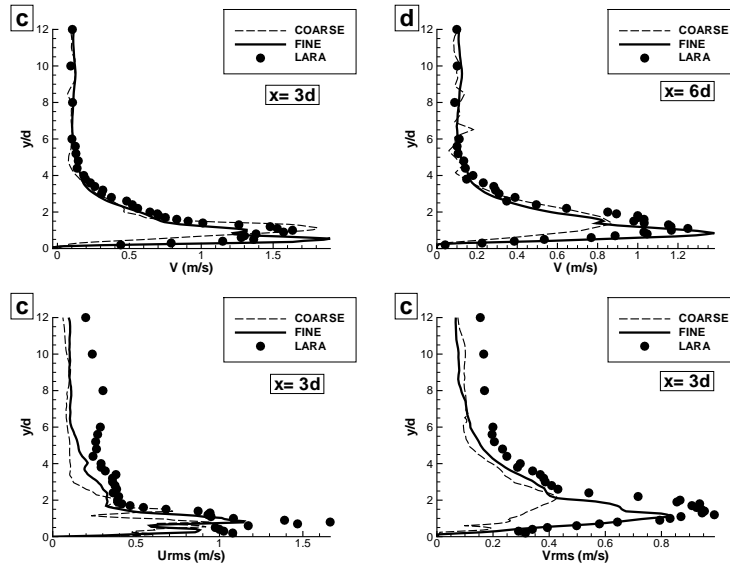


Fig. 6. Validation of the calculations on different quantities: dotted lines correspond to LES results with the coarse grid, continuous line to LES with the finer grid and symbols correspond to measurements. TOP: Mean vertical velocity profiles at two locations downstream of the jet. BOTTOM: Root Mean Square streamwise and vertical velocity at station c.

This confirms that the effusion process is well reproduced with the fine grid and that the differences between experimental and numerical results are mainly due to the difference between a finite and an infinite perforated plate.

4.3 General Features Of The Flow

Numerical simulations are also able to provide information that are difficult to obtain from experimental measurements, like the topology of the flow in the hole or wall shear stress maps over the cooled wall.

Behavior In The Hole

The topology of the flow in the hole starts to be known thanks to numerical studies that have confirmed assumptions made by experimenters. Figure 7 shows fields of mean streamwise velocity in the hole.

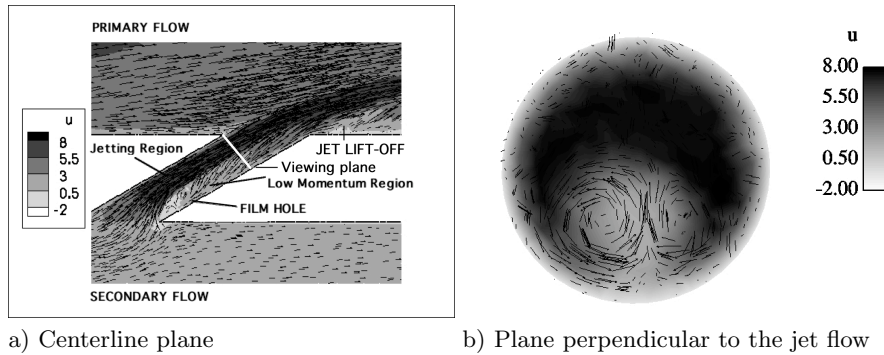


Fig. 7. Computed mean streamwise velocity (in m/s) and velocity vectors in the hole.

The flow computed in the case of short holes with high blowing ratios is complex. Figure 7 allows to observe trends that have already been detected by Leylek and Zerkle [19] and by Walters and Leylek [20, 21] on a similar configuration thanks to RANS calculations: the jet separates at the entry of the hole (Fig. 7.a) and two different regions can be defined: the jetting region, near the upstream wall of the hole, where the jet shows high velocities, and the low-momentum region. As the length of the holes is small, the jet at the exit of the hole is still highly influenced by what happens at the entry of the hole. Figure 7.b also shows that two counter rotating vortices are present in the hole itself. The sense of rotation of these vortices is the same as for the classical counter rotating vortex pair that is observed in jets in crossflow studies (see [22]). Here it can be noticed again that, as suggested earlier by

many authors, a strong interaction between the secondary flow, the film-hole and the primary flow exists and has to be reproduced to be representative for gas turbines cooling applications.

Wall Shear Stress

Numerical studies can easily provide information about the wall shear stress. Even if the refinement at the wall is not optimal (the first off-wall point is situated at $y^+ \approx 5$), reasonable assessment of the shear stress at the wall is expected from the LES. Figure 8 shows the mean shear stress at the wall that has to be cooled. It shows the main aspects of the near-wall flow:

- High values of wall shear stress (approximately 0.2 N.m^{-2}) can be observed on the sides of the hole and just downstream. They are signs of the entrainment process. Here, the flow is deflected towards the wall and particles with high velocities go close to the wall, generating high shear.
- Downstream of the hole, a zone of low values (approximately 0.05 N.m^{-2}) shows the presence of the jet lift-off just after the hole. Moreover, the jet plays the role of an obstacle for the incident flow.
- On the remaining of the plate, the wall shear stress appears to be quite homogeneous.

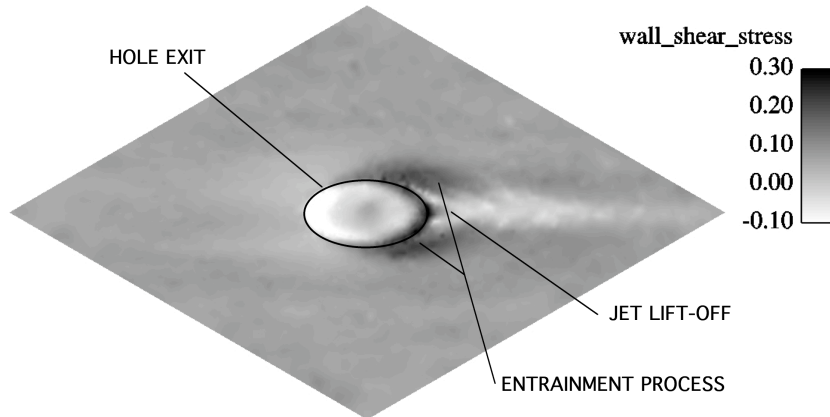


Fig. 8. Wall shear stress (in N.m^{-2}) map on the "combustion chamber" side of the wall.

Figure 8 also allows to understand the contribution of the jet to the wall shear stress: even if the contribution of the hole region on this plane is not very

high, disturbances of the near-wall region due the jet are very important. The shear stress at the wall is not constant any more, like over an impermeable plate: the jet has a strong effect on the topology of the flow, noticeably by creating locally high and low shear stress regions. The flow in the near-wall region appears to be far too complicated to be modeled by a classical log-law or by a law that takes into account the porosity of the plate by introducing a scaling factor in the classical log-law.

5 Conclusion

To compute realistic cases of effusion cooling for combustion chamber liners, the generic configuration of an infinite perforated plate has been chosen. The method proposed to generate the flow in a periodic configuration (infinite plate reduced to a domain containing one single hole with periodic boundary conditions in the tangential directions) provides interesting results. They are compared to an experimental database on a large-scale isothermal configuration.

Several comments can be made:

- The velocity field in the jet shows a realistic form: separation of the jet due to the sharp-edged, inclined inlet along the downstream portion of the hole is reproduced.
- At the outlet of the hole, the jet lift-off and the entrainment process are observed.
- Good general agreement with experimental measurements is observed. Velocity gradients at the wall are correctly predicted. The mean streamwise velocity shows an effect of the infinite plate, with differences on the film core prediction, compared to the experimental data.
- RMS velocity levels show a good general behavior, with good levels of turbulent intensities near the wall ($y/d < 4$).

The isothermal configuration is the first step of the work on effusion cooling modeling. In order to study the heat transfer on the multi-perforated plate, the method presented in this article should be adapted to compute Large-Eddy Simulations of a non-isothermal flow.

Acknowledgements

The authors are grateful to the European Community for funding this work under the project INTELLECT-DM (Contract No. FP6 - AST3 - CT - 2003 - 502961), and to the CINES (Centre Informatique National pour l'Enseignement Supérieur) for the access to supercomputer facilities. The authors also acknowledge TURBOMECA for allowing the use of the two snapshots displayed in Fig. 1.

References

- [1] P. Miron: (2005), “Étude expérimentale des lois de parois et du film de refroidissement produit par une zone multiperforée sur une paroi plane.”, Ph.D. thesis, Université de Pau et des Pays de l’Adour
- [2] A.H. Lefebvre: *Gas Turbines Combustion* (Taylor & Francis, 1999)
- [3] R. Goldstein: *Advances in Heat Transfer* (Academic Press, New-York and London, 1971)
- [4] K.M.B. Gustafsson: (2001), “Experimental studies of effusion cooling”, Ph.D. thesis, Chalmers University of Technology. Goteborg
- [5] S. Yavuzkurt, R. Moffat, W. Kays: *J. Fluid Mech* **101**, 129–158 (1980)
- [6] F. Bazdidi-Tehrani, G. Andrews: *Journal of Engineering for Gas Turbines and Power* **116**, 587–596 (1994)
- [7] S. Rouvreau: (2001), “Étude expérimentale de la structure moyenne et instantanée d’un film produit par une zone multiperforée sur une paroi plane. application au refroidissement des chambres de combustion des moteurs aeronautiques”, Ph.D. thesis, E.N.S.M.A. et Faculté des Sciences Fondamentales et Appliquées
- [8] M.K. Harrington, M.A. McWaters, D.G. Bogard, L.C. A., K.A. Thole: *ASME TURBOEXPO 2001*. 2001-GT-0130 (2001)
- [9] E. Papanicolaou, D. Giebert, R. Koch, A. Schultz: *International Journal of Heat and Mass Transfer* **44**, 3413–3429 (2001)
- [10] M. Tyagi, S. Acharya: *Journal of Turbomachinery* **125**, 734–742 (2003)
- [11] L.L. Yuan, R.L. Street, J.H. Ferziger: *J. Fluid Mech.* **379**, 71–104 (1999)
- [12] P. Moin, K. Mahesh: *Annu. Rev Fluid Mech.* **30**(539-578) (1998)
- [13] S. Mendez, F. Nicoud, P. Miron: “Direct and large-eddy simulations of a turbulent flow with effusion”, in *ERCOFTAC WORKSHOP. Direct and Large-Eddy Simulations 6. Poitiers FRANCE* (2005)
- [14] T. Poinsot, S. Lele: *J. Comp. Physics* **vol.101**(1), 104–129 (1992)
- [15] V. Moureau, G. Lartigue, Y. Sommerer, C. Angelberger, O. Colin, T. Poinsot: *J. Comp. Physics* **202**(2), 710–736 (2005)
- [16] F. Nicoud, F. Ducros: *Flow, Turbulence and Combustion* **62**(3), 183–200 (1999)
- [17] O. Colin, M. Rudgyard: *J. Comp. Physics* **162**(2), 338–371 (2000)
- [18] P. Miron, C. Berat, V. Sabelnikov: “Effect of blowing rate on the film cooling coverage on a multi-holed plate: application on combustor walls”, in *Eighth International Conference on Heat Transfer. Lisbon, Portugal* (2004)
- [19] J. Leylek, R.D. Zerkle: *Journal of Turbomachinery* **116**, 358–368 (1994)
- [20] D. Walters, J. Leylek: *Journal of Turbomachinery* **119**, 777–785 (1997)
- [21] D. Walters, J. Leylek: *Journal of Turbomachinery* **122**, 102–112 (2000)
- [22] J. Andreopoulos, W. Rodi: *J. Fluid Mech* **138**, 93–127 (1984)